

IMMUNOLOGY

The regulatory B cell-mediated peripheral tolerance maintained by mast cell IL-5 suppresses oxazolone-induced contact hypersensitivity

Hyuk Soon Kim^{1*}, Min Bum Lee^{1*}, Dajeong Lee¹, Keun Young Min¹, Jimo Koo¹, Hyun Woo Kim¹, Young Hwan Park¹, Su Jeong Kim¹, Masashi Ikuuti², Satoshi Takaki², Young Mi Kim³, Wahn Soo Choi^{1†}

The function of regulatory immune cells in peripheral tissues is crucial to the onset and severity of various diseases. Interleukin-10 (IL-10)-producing regulatory B (IL-10⁺ B_{reg}) cells are known to suppress various inflammatory diseases. However, evidence for the mechanism by which IL-10⁺ B_{reg} cells are generated and maintained is still very limited. Here, we found that IL-10⁺ B_{reg} cells suppress the activation of IL-13-producing type 2 innate lymphoid cells (IL-13⁺ ILC2s) in an IL-10-dependent manner in mice with oxazolone-induced severe contact hypersensitivity (CHS). Mast cell (MC) IL-5 was important for maintaining the population of IL-10⁺ B_{reg} cells in peripheral lymphoid tissues. Overall, these results uncover a previously unknown mechanism of MCs as a type of immunoregulatory cell and elucidate the cross-talk among MCs, IL-10⁺ B_{reg} cells, and IL-13⁺ ILC2s in CHS.

INTRODUCTION

B cells are known for their capacity to produce antibodies and to stimulate helper T cells as antigen-presenting cells (APCs) (1), and these B cells are commonly referred to as conventional B cells or B-2 cells. However, some unique B cell subsets can suppress various immune responses. Katz and co-workers (2) were the first to demonstrate that the delayed-type hypersensitivity reaction was aggravated by the depletion of B cells. After 30 years, Mizoguchi and Bhan (3) introduced the term regulatory B (B_{reg}) cells to designate negative regulatory B cell subsets. Subsequently, many studies have reported that B_{reg} cells suppress various immune disorders, such as collagen-induced arthritis, experimental autoimmune encephalomyelitis, contact hypersensitivity (CHS), and colitis (4). Although the inhibitory mechanism of B_{reg} cells is mostly interleukin-10 (IL-10) dependent, B_{reg} cells can also regulate the immune response by secreting transforming growth factor-β (TGF-β) or IL-35. TGF-β⁺CD5⁺ B cells induce the development of Foxp3⁺ regulatory T (T_{reg}) cells to suppress allergic airway inflammation (5). IL-35 secreted by B_{reg} cells not only inhibited T helper cell 1 (T_H1)/T_H17 immunity but also increased the population of T_{reg} cells to inhibit experimental autoimmune uveitis (4). The knockout of IL-35 in B cells also resulted in enhanced T_H1 cell responses in autoimmune and infectious diseases (6). In another mechanism, programmed death-ligand 1 (PD-L1)^{hi} B cells inhibited the development of follicular T cells by direct contact with PD-1 on the surface of activated T cells (7). However, information about how B_{reg} cells are developed and maintained in peripheral tissues to regulate inflammatory diseases is very limited.

Mast cells (MCs) are essential cells for inducing immediate hypersensitivity (also known as type I hypersensitivity) through immunoglobulin E (IgE)-bound high-affinity Fc epsilon Receptor I (FcεRI)

signaling (8). When MCs are activated by antigen, preformed granules that contain histamine and other proinflammatory mediators, eicosanoids, and proinflammatory cytokines are released from MCs. Because of the sustained release of these mediators, MCs are also known to be the major effector cells in immediate- and delayed-type hypersensitivity. In particular, MCs are activated by antigen or various stimulants in the state of allergic diseases, such as atopic dermatitis, allergic rhinitis, asthma, and anaphylaxis, thereby increasing the severity of the disease (8). On the contrary, recent studies have shown some interesting results regarding the inhibitory role of MCs in hypersensitivity-related immune responses. We and others reported that MCs increase the population of IL-10-producing B_{reg} cells in vitro and in vivo (9, 10). In the type I hypersensitivity immune response, the CD40 ligand of MCs stimulates B_{reg} cell development by interacting with CD40 of CD5⁺ B-1a cells as a negative regulatory mechanism of MCs (9). However, the mechanism of IL-10⁺ B_{reg} cell development by MCs in peripheral tissues has not been established.

CHS is a representative type of T_H1 immunity-associated allergic skin inflammation. The process of CHS is divided into two distinct phases. During sensitization, haptens are taken up by APCs, such as Langerhans cells and dermal dendritic cells. In the draining lymph node (LN), migrating APCs activate antigen-specific T cells (11). It has been reported that CD1d⁺ APCs, IL-4-producing natural killer T cells, and IgM from peritoneal B-1 cells also participate in the sensitization phase (12). In the elicitation phase, the hapten-specific T cells migrate to the inflammatory site. These cells release various proinflammatory cytokines and chemokines, leading to leukocyte infiltration. Overall, although hapten-induced T_H1 responses are predominant, T_H2 mediators are also activated during the response and contribute substantially to the pathology of CHS (12). Repeated challenges with OXZ in mice result in chronic allergic inflammatory responses similar to those observed in human atopic dermatitis, such as barrier disruption, T_H2 cell-predominant inflammation, and hyper-infiltration of other effector cells, such as MCs and eosinophils (13). However, some studies have unexpectedly presented results regarding the inhibitory role of MCs in CHS (14–17). In severe CHS, MCs suppress the development of skin inflammation through the secretion of IL-10 (14, 17).

Copyright © 2019
The Authors, some
rights reserved;
exclusive licensee
American Association
for the Advancement
of Science. No claim to
original U.S. Government
Works. Distributed
under a Creative
Commons Attribution
NonCommercial
License 4.0 (CC BY-NC).

¹Department of Immunology, School of Medicine, Konkuk University, Chungju 27478, Korea. ²Department of Immune Regulation, The Research Center for Hepatitis and Immunology, Research Institute, National Center for Global Health and Medicine, Chiba 272-8516, Japan. ³Department of Preventive Pharmacy, College of Pharmacy, Duksung Women's University, Seoul 01369, Korea.

*These authors contributed equally to this work.

†Corresponding author. Email: wahnchoi@kku.ac.kr

or through the expansion of T_{reg} cells by IL-2 released from MCs (15). These studies further suggest that there exists another regulatory mechanism that remains to be clear.

The group 2 innate lymphoid cells (ILC2s) have emerged as potent effector cells in various allergic diseases, including skin inflammation. Similar to T_{H2} cells, ILC2s secrete type 2 cytokines, such as IL-4, IL-5, and IL-13. These cells are known to be involved in initial host defense and parasitic infection, but recent studies have shown that they also play a critical role in causing allergic symptoms in atopic dermatitis and allergic asthma (18). In particular, IL-13 is known to play a key role in skin fibrosis and epithelial disruption, and ILC2s have further been demonstrated to be a major source of IL-13 in skin pathology (19). Although many studies on the function of ILC2s have been reported in hypersensitivity-related skin inflammation, including atopic dermatitis, little is known about the regulation of ILC2s in peripheral tissues.

In this study, we demonstrate that $IL-10^+ B_{reg}$ cells suppress $IL-13^+ ILC2s$ to inhibit CHS in an IL-10-dependent manner. Furthermore, MC IL-5 is important for the maintenance of $IL-10^+ B_{reg}$ cells in peripheral lymphoid tissues.

RESULTS

Population changes in MCs, ILC2s, and B_{reg} cells in lymphoid tissues of mice with oxazolone-induced CHS

To analyze the alterations of various immune cells in CHS, we induced severe CHS by oxazolone (OXZ) in mice (Fig. 1, A and B) and examined the distributions of MCs, ILC2s, and $IL-10^+ B_{reg}$ cells in spleen, axillary LN (aLN), inguinal LN (iLN), peritoneal cavity (PeC), and ear (Fig. 1). The populations of immune cells, such as $CD4^+ T$ cells, neutrophils, monocytes/macrophages, and dendritic cells, that are responsible for local inflammation increased mostly in the draining LNs and ear tissue of CHS mice (fig. S1). MCs were frequently detected in the LNs and ear tissue but rarely detected in the spleen (Fig. 1C). While the number of MCs in the LNs was decreased by the induction of CHS, MCs were increased in the ear tissue (Fig. 1D). The number of $IL-13^+ ILC2s$ was increased in the spleen, LNs, and ear tissue during CHS (Fig. 1, E and F), suggesting the possibility that $IL-13^+ ILC2s$ are also associated with the pathology of OXZ-induced CHS. We further observed that the number of $IL-10^+ B_{reg}$ cells was also increased in the spleen and LNs but not in the PeC (Fig. 1, G and H). In some allergic diseases, such as casein-induced food allergy, the inhibitory effect of $IL-10^+ B_{reg}$ cells is T_{reg} cell dependent (20). However, the generation of $IL-10^+ B_{reg}$ cells in OXZ-induced CHS was induced regardless of the presence of T_{reg} cells (fig. S2). It was reported that most $IL-10^+ B_{reg}$ cells are derived from $CD1d^{hi}CD5^+ B_{reg}$ precursor cells in CHS mice (21). The number of $CD1d^{hi}CD5^+ B$ cell subsets was accordingly increased in the LNs but not in the spleen and PeC in CHS mice (Fig. 1, I and J). We further observed that the changes in immune cell populations were similar in mice with chronic atopic dermatitis-like symptom induced by OXZ (fig. S3). These results led us to conduct a study of the cross-talk among MCs, $IL-10^+ B_{reg}$ cells, and $IL-13^+ ILC2s$ in peripheral lymphoid tissues during CHS.

The suppressive effect of B_{reg} cells on $IL-13^+ ILC2s$ is independent of T_{reg} cells but dependent on IL-10

In our previous study, we reported that $IL-10^+ B_{reg}$ cells inhibit MC activity in mice with IgE-mediated anaphylaxis (9). Yanaba and co-workers reported that CHS is exacerbated in CD19-deficient mice,

in which $IL-10^+ B_{reg}$ cells are mostly depleted (21). Notably, the symptoms were more severe in CD19-deficient mice than in wild-type (WT) mice (Fig. 2A), suggesting that $IL-10^+ B_{reg}$ cells are important for suppressing CHS. Compared to that in WT mice, the number of $IL-13^+ ILC2s$ was substantially increased in the aLN and ear tissue but not in the spleen in CD19-deficient mice (Fig. 2B), suggesting that $IL-13^+ ILC2s$, which could be associated with the induction of CHS, are inhibited by B_{reg} cells. However, we did not observe any difference in the number of MCs between WT and CD19-deficient mice during CHS (fig. S4A). In addition, we could not find any difference in the distribution of $CD4^+ T$ cells, $Foxp3^+ T_{reg}$ cells, and $IL-10^+ T_{reg}$ cells (Tr1) in the spleen, LN, or ear tissue of CD19-deficient CHS mice, suggesting that $IL-13^+ ILC2s$ are likely to be controlled by B_{reg} cells in the OXZ-induced CHS (fig. S4, B to D). To test this hypothesis, we adoptively transferred $CD1d^{hi}CD5^+ B$ cells containing $IL-10^+ B_{reg}$ cells into CD19-deficient mice. The adoptive transfer of $CD1d^{hi}CD5^+ B$ cells but not $Il10^{-/-} CD1d^{hi}CD5^+$ or non- $CD1d^{hi}CD5^+ B$ cells significantly suppressed CHS symptoms (Fig. 2C). These results indicate that $IL-10^+ B_{reg}$ cells play a pivotal role in the inhibition of CHS. Furthermore, the adoptive transfer of $CD1d^{hi}CD5^+ B$ cells but not $Il10^{-/-} CD1d^{hi}CD5^+$ or non- $CD1d^{hi}CD5^+ B$ cells inhibited the number of $IL-13^+ ILC2s$ in LNs and ear tissue in CD19-deficient CHS mice (Fig. 2D). These results indicate that B_{reg} cells inhibit $IL-13^+ ILC2s$ in an IL-10-dependent manner to suppress the OXZ-induced CHS response in mice.

OXZ-induced CHS is generally accepted as a T cell-dependent response (22). To eliminate the roles of effector and T_{reg} cells in OXZ-induced CHS mice, we next used $Rag2^{-/-}$ mice in which B cells and T cells are mostly depleted (23). However, the $IL-13^+ ILC2$ population was still intact (Fig. 2E), and OXZ-induced CHS was evident in $Rag2^{-/-}$ mice (Fig. 2F), indicating that the OXZ-induced CHS response is induced in the absence of T cells. When total ILCs were depleted by the administration of a Thy1.2 monoclonal antibody (mAb) in $Rag2^{-/-}$ mice, the CHS response induced by OXZ was significantly suppressed (Fig. 2, F and G). Furthermore, the response was significantly reduced when we administered anti-IL-13 antibody into OXZ-induced CHS mice (fig. S5), indicating that the IL-13 secretion of ILC2s is closely associated with the CHS response induced by OXZ. $IL-10^+ B_{reg}$ cells were reconstituted in the spleen and LN but not in the ear tissues after the adoptive transfer of $CD19^+ B$ cells (Fig. 2H). The OXZ-induced CHS response in $Rag2^{-/-}$ mice was significantly inhibited by the adoptive transfer of WT $CD1d^{hi}CD5^+ B$ cells but not $Il10^{-/-} CD1d^{hi}CD5^+ B$ cells (Fig. 2I). Furthermore, the number of $IL-13^+ ILC2s$ was also decreased in the LNs and ear tissue after the adoptive transfer of WT $CD1d^{hi}CD5^+ B$ cells but not $Il10^{-/-} CD1d^{hi}CD5^+ B$ cells (Fig. 2J). These results again suggest that B_{reg} cells inhibit $IL-13^+ ILC2s$ in an IL-10-dependent manner. Next, we conducted an in vitro coculture experiment to evaluate the inhibition of $IL-13^+ ILC2s$ by B_{reg} cells. WT $CD1d^{hi}CD5^+ B$ cells but not WT non- $CD1d^{hi}CD5^+$ or $Il10^{-/-} CD1d^{hi}CD5^+ B$ cells significantly inhibited the expression of IL-13 in ILC2s (Fig. 2, K and L). These results further suggest that B_{reg} cell-derived IL-10 inhibits the activation of ILC2s to secrete IL-13 in OXZ-induced CHS mice.

MCs are critical for the enhancement of $IL-10^+ B_{reg}$ cells in peripheral tissues

In some previous studies, MCs were reported as negative regulators of CHS disease. The production of IL-10 by dermal MCs contributes to the anti-inflammatory effects of MCs in allergic contact dermatitis (14).

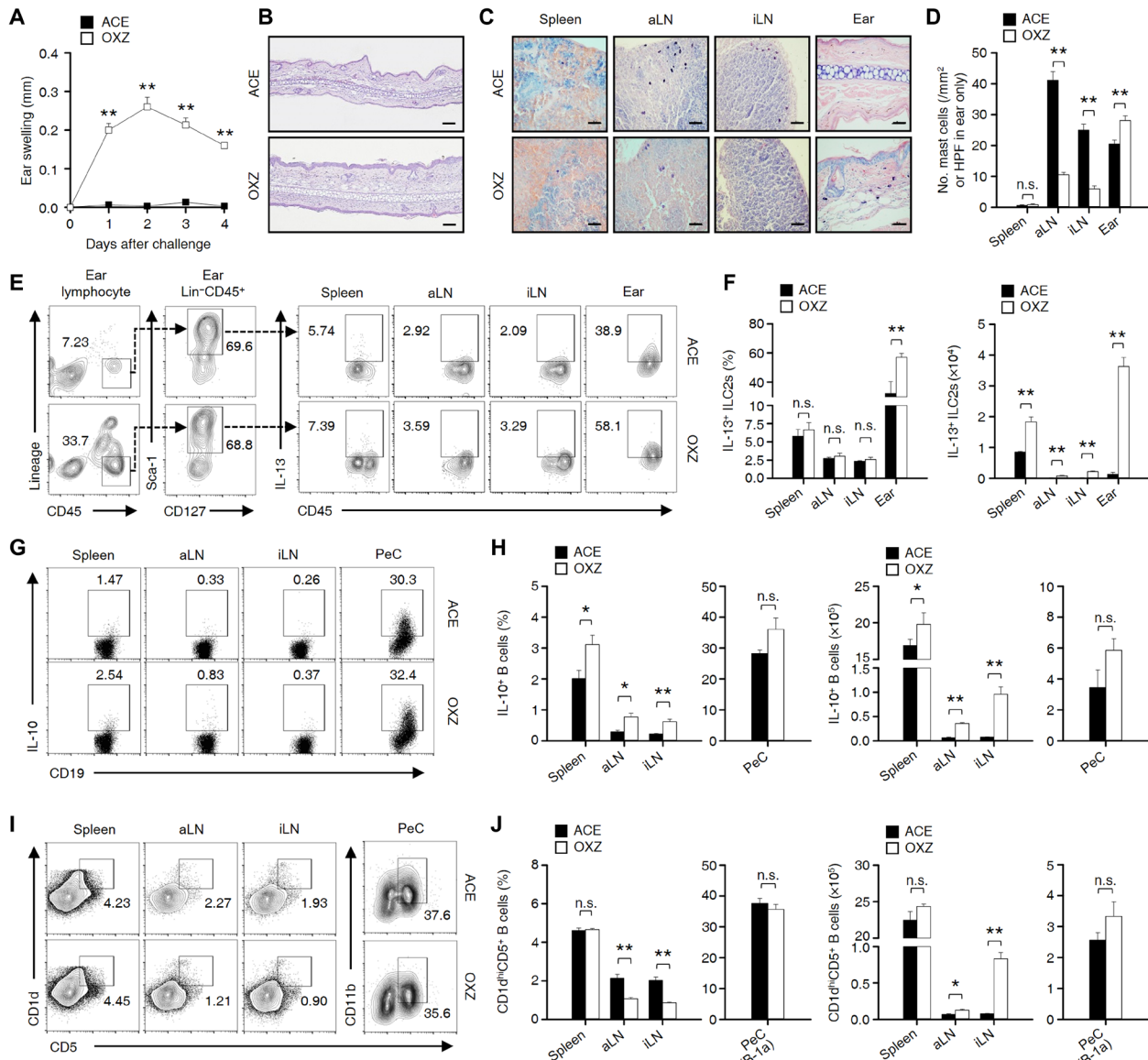


Fig. 1. Population alterations of MCs, ILC2s, and IL-10⁺ B_{reg} cells in CHS mice. (A) Data for the ear thickness of CHS mice for 4 days after challenge with OXZ are shown. (B) Two days after OXZ challenge, representative histology images of ear tissues [hematoxylin and eosin (H&E); scale bars, 200 μ m] are shown. (C) Two days after OXZ challenge, representative MC images in spleen, aLN, iLN (scale bars, 50 μ m), and ear tissues [high-power field (HPF); scale bar, 100 μ m] with toluidine blue are shown, and (D) the histograms show the number of MCs in spleen, aLN, iLN, and ear tissues. (A to D) The results are expressed as the mean \pm SEM (A and D) or representative images (B and C) from three independent experiments ($n=5$ per group for each experiment). ** $P < 0.01$; n.s., not significant versus ACE-treated mice by Student's *t* test. (E) Representative plot images show IL-13⁺Lin⁻CD45⁺CD127⁺Sca-1⁺ cells (IL-13⁺ ILC2s) in spleen, aLN, iLN, and ear. (F) The histograms show the frequencies and numbers of IL-13⁺ ILC2s for (E). (G) Representative flow cytometry images are shown for IL-10⁺CD19⁺ B cells or (I) CD1d^{hi}CD5⁺CD19⁺ B cells in the spleen, aLN, and iLN or CD5⁺CD11b⁺CD19⁺ B cells in the PeC. (H) Frequencies and numbers are shown for (G) and (J) for (I). (E to J) The results are expressed as representative images (E, G, and I) or the mean \pm SEM (F, H, and J) from two independent experiments ($n=5$ per group for each experiment). * $P < 0.05$; ** $P < 0.01$; n.s., not significant versus acetone (ACE)-treated mice by Student's *t* test.

It was also reported that MC-derived IL-2 contributes to the suppression of chronic allergic skin inflammation via the induction of Foxp3⁺ Treg cells (15). MCs also stimulate the expansion and differentiation of IL-10⁺ B_{reg} cells in colitis (10) and IgE-mediated anaphylaxis (9). However, it remains totally unclear how MCs stimulate the IL-10⁺ B_{reg} cell population. We observed that the CHS response was markedly increased in MC-deficient *Kit*^{W-sh/W-sh} mice compared to that in WT mice (Fig. 3, A and B). Notably, the frequency and number of IL-10⁺ B_{reg} cells were significantly reduced in the spleen, aLN, iLN,

and PeC in MC-deficient *Kit*^{W-sh/W-sh} mice (Fig. 3, C and D), but no significant changes in the total B cell population were observed in the spleen, aLN, iLN, or PeC (fig. S6A). In the comparative experiment of WT and *Kit*^{W-sh/W-sh} mice, the expressions of surface proteins from splenic B cells were not changed, if any, marginally changed, but those from PeC showed some changes (fig. S6B). We and other researchers have assumed that these changes have occurred because of the high proportion, approximately 40%, of IL-10⁺ B-1a cell population in PeC B cells (21). Notably, there was no change in the serum concentration

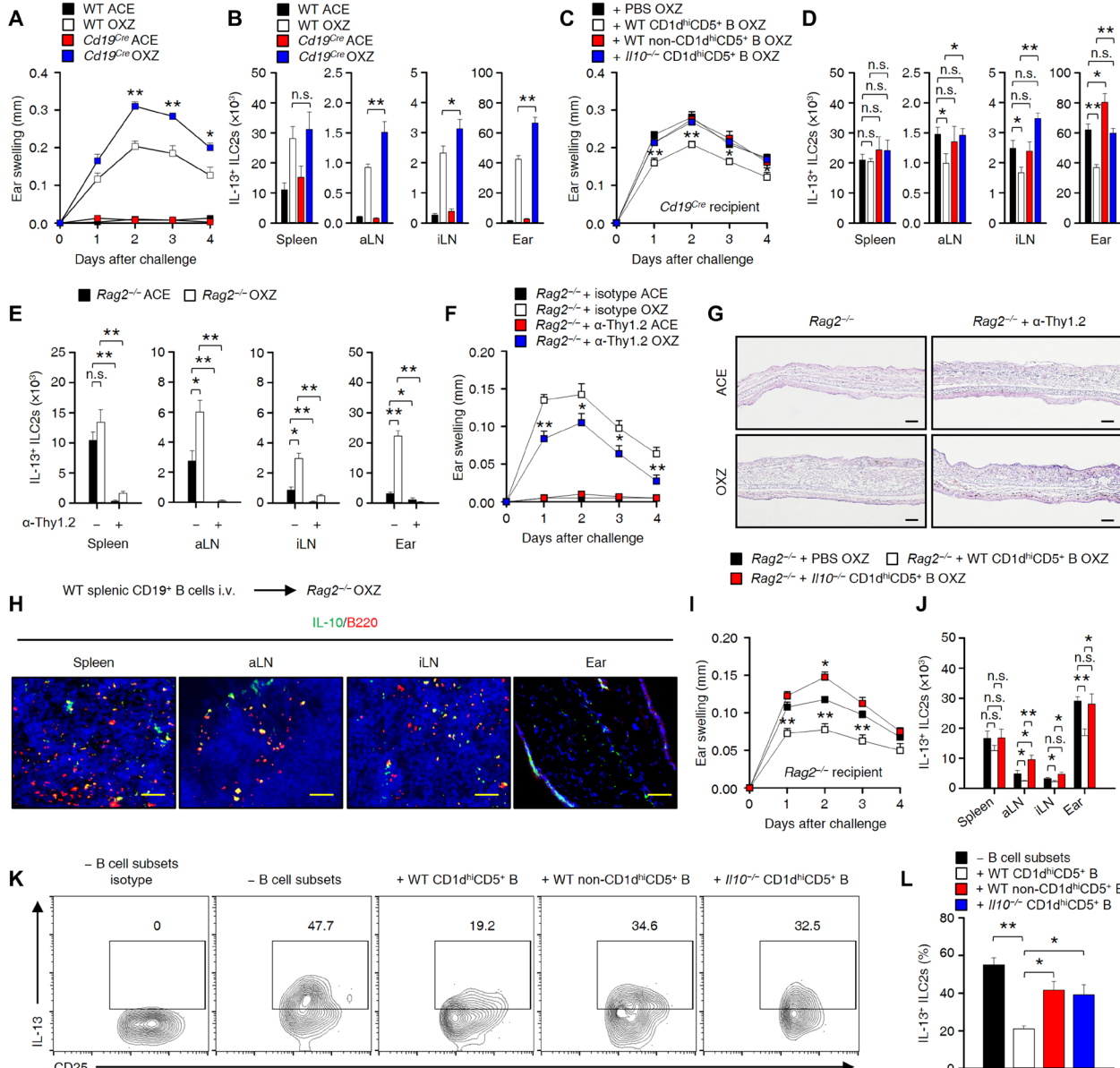


Fig. 2. B_{reg} cells suppress IL-13⁺ ILC2s in an IL-10-dependent manner. (A) Data for the ear thickness of WT or Cd19^{Cre} mice with CHS for 4 days after challenge with OXZ are shown. (B) The histograms show the numbers of IL-13⁺ ILC2s isolated from the spleen, aLN, iLN, and ear tissue 2 days after the OXZ challenge. (C) Data for the ear thickness and (D) the number of IL-13⁺ ILC2s in Cd19^{Cre} mice with CHS are shown after the adoptive transfer of OXZ-sensitized WT or /I10^{-/-} B cell subsets as indicated. (A to D) The results are expressed as the mean ± SEM from two independent experiments ($n = 5$ per group for each experiment). * $P < 0.05$; ** $P < 0.01$; n.s., not significant by Student's *t* test (A to C) or one-way analysis of variance (ANOVA) with post hoc Tukey's test (D). (E to G) The histograms for (E) the number of tissue IL-13⁺ ILC2s, (F) the ear thickness, and (G) the histology images of ear tissues (2 days after OXZ challenge; scale bars, 200 μ m) in CHS Rag2^{-/-} mice with or without anti-Thy1.2 mAb treatment are shown. The results are expressed as the mean ± SEM from two independent experiments ($n = 4$ per group for each experiment). * $P < 0.05$; ** $P < 0.01$; n.s., not significant versus Rag2^{-/-} + isotype OXZ by Student's *t* test. (H) After the adoptive transfer of WT splenic CD19⁺ B cells into Rag2^{-/-} mice, CHS was induced by OXZ challenge. Representative immunofluorescence images of IL-10 (green) and B220 (red) are shown ($n = 5$; scale bars, 100 μ m). (I) Ear thicknesses and (J) IL-13⁺ ILC2 numbers in CHS Rag2^{-/-} mice with or without the transfer of WT or /I10^{-/-} CD1d^{hi}CD5⁺ B cell subsets. (K) Representative flow cytometry images for IL-13⁺ ILC2s in coculture with WT CD1d^{hi}CD5⁺, WT non-CD1d^{hi}CD5⁺, or /I10^{-/-} CD1d^{hi}CD5⁺ B cell subsets at a 1:1 ratio and (L) frequency data are shown. (I to L) The results are expressed as the mean ± SEM (I, J, and L) or representative images (K) from two independent experiments ($n \geq 3$ per group for each experiment). * $P < 0.05$; ** $P < 0.01$; n.s., not significant by Student's *t* test (I) or one-way ANOVA with post hoc Tukey's test (J and L).

of four isotypes of antibody (fig. S6C), and we did not observe any difference in the frequency of IL-10⁺ B_{reg} cells from bone marrow in between WT and Kit^{W-sh/W-sh} mice (fig. S6D). Such an observation suggested that MCs play an important role in maintaining the ho-

meostasis of IL-10⁺ B_{reg} cells in the peripheral tissues but not in the bone marrow.

ILC2s have been reported to be a type of effector cell in skin inflammatory disorders, including atopic dermatitis (19, 24). In our study,

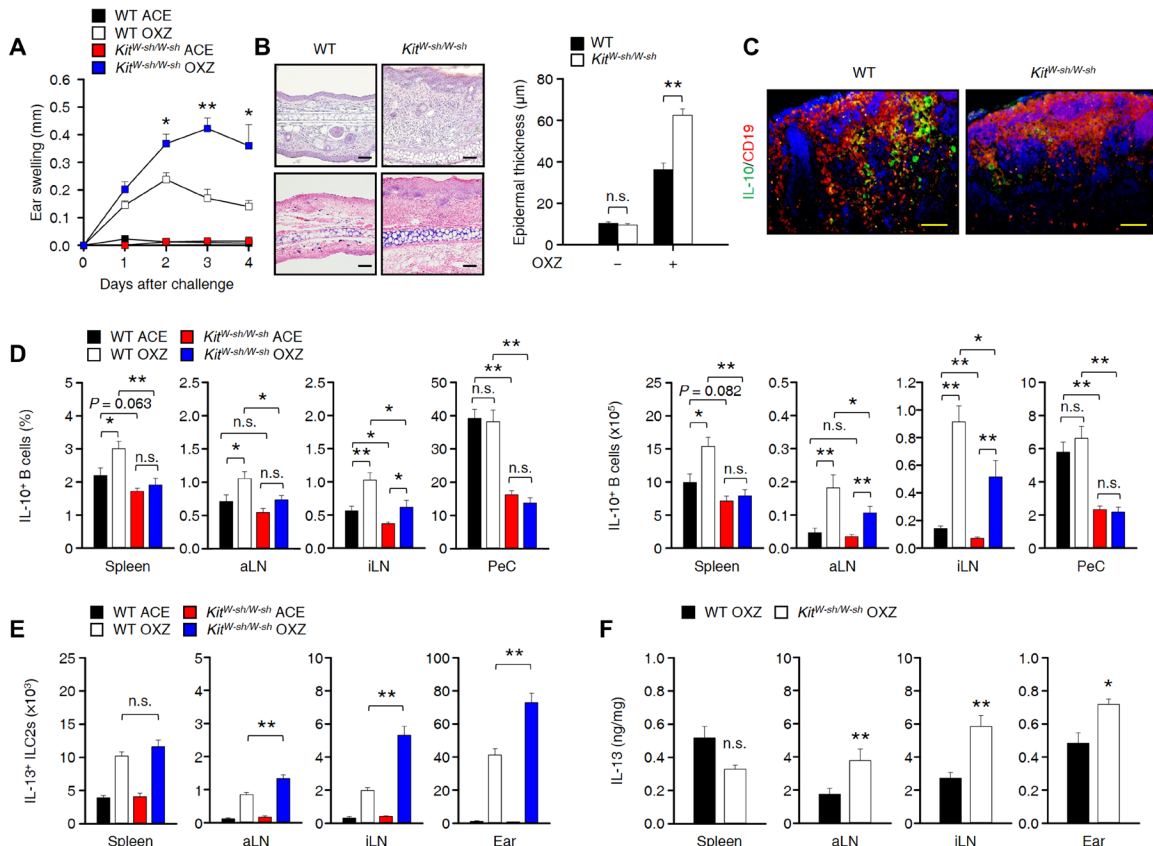


Fig. 3. MCs are critical for the maintenance of IL-10⁺ B_{reg} cells and the inhibition of IL-13⁺ ILC2s in peripheral tissues. (A) Ear thickness is shown for 4 days after challenge with OXZ in WT or *Kit*^{W-sh/W-sh} mice. (B) Representative images (2 days after OXZ challenge) after staining with H&E (top) or toluidine blue (bottom) of ear tissues (scale bars, 100 μ m) and histograms of ear epidermal thickness are shown. (A and B) Data are expressed as the mean \pm SEM from three independent experiments ($n \geq 4$ per group for each experiment). * $P < 0.05$; ** $P < 0.01$; n.s., not significant by Student's *t* test. (C) Representative immunofluorescence images of IL-10⁺ B_{reg} cells in the draining LNs from WT and *Kit*^{W-sh/W-sh} mice are shown (IL-10, green; CD19, red) ($n = 5$; scale bars, 50 μ m). (D to F) The results from tissues of WT or *Kit*^{W-sh/W-sh} mice 4 days after challenge with OXZ are shown. (D) The histograms show the frequencies (left) and numbers (right) of IL-10⁺ B_{reg} cells. (E) The histograms show the numbers of IL-13⁺ ILC2s. (F) The histograms show the amount of IL-13 by enzyme-linked immunosorbent assay (ELISA). (D to F) Data are expressed as the mean \pm SEM from two independent experiments ($n \geq 3$ per group for each experiment). * $P < 0.05$; ** $P < 0.01$; n.s., not significant by one-way ANOVA with post hoc Tukey's test.

the population of IL-13⁺ ILC2s and the amount of secreted IL-13 were greatly increased in the LNs and ear tissue of *Kit*^{W-sh/W-sh} mice (Fig. 3, E and F). Notably, no defect in intrinsic IL-10⁺ Tr1 and Foxp3⁺ T_{reg} cells was found in *Kit*^{W-sh/W-sh} mice compared to WT mice (fig. S6, E and F). These results suggest that MCs are critical for the maintenance of IL-10⁺ B_{reg} cells, which suppress IL-13⁺ ILC2s in the peripheral tissues of mice with CHS.

Reconstitution of MCs restores the population of IL-10⁺ B_{reg} cells in MC-deficient *Kit*^{W-sh/W-sh} mice

We next found that the population of IL-10⁺ B_{reg} cells in the peripheral tissues was diminished (Fig. 3D), but IL-13⁺ ILC2s were increased in *Kit*^{W-sh/W-sh} mice compared to those in WT mice (Fig. 3E). Notably, the severity of the CHS response was augmented in *Kit*^{W-sh/W-sh} mice compared to that in WT mice (Fig. 3A). These results suggest that MCs can stimulate the development of IL-10⁺ B_{reg} cells in peripheral lymphoid tissues and that IL-10⁺ B_{reg} cells suppress the CHS response by inhibiting IL-13⁺ ILC2s. To further investigate the mechanism by which MCs stimulate the development of IL-10⁺ B_{reg} cells, we tested the relationship between CHS severity and the development of IL-10⁺ B_{reg} cells by MC reconstitution in *Kit*^{W-sh/W-sh} mice. The total popula-

tion of CD19⁺ B cells in the peripheral tissues showed no differences between WT and *Kit*^{W-sh/W-sh} mice with or without reconstitution of MCs (Fig. 4A). However, the populations of IL-10⁺ B_{reg} cells and CD5⁺ B cells in the LNs, spleen, and PeC were restored by the reconstitution of MCs (Fig. 4, B and C), suggesting that MCs could stimulate the population of IL-10⁺ B_{reg} cells by stimulating the development of B_{reg} precursor cells. When MCs were reconstituted intravenously (i.v.) in *Kit*^{W-sh/W-sh} mice, IL-10⁺ B_{reg} cells in the LNs and spleen but not the PeC were restored, and only PeC IL-10⁺ B-1a cells were recovered by the intraperitoneal (i.p.) transfer of MCs (Fig. 4B). Furthermore, we observed that CHS responses were significantly suppressed in MC-reconstituted *Kit*^{W-sh/W-sh} mice compared to those in *Kit*^{W-sh/W-sh} mice (Fig. 4D). Suppression of the CHS response was observed only when MCs were reconstituted intravenously but not intraperitoneally (fig. 4D), suggesting that the restoration of IL-10⁺ B_{reg} cells in the LNs or spleen, but not PeC, by MCs plays a critical role in the suppression of the CHS response (Fig. 4E). Notably, the number of IL-13⁺ ILC2s was suppressed in the LNs and ear tissue of MC-reconstituted mice compared to that in MC-deficient *Kit*^{W-sh/W-sh} mice (Fig. 4F). These results suggest that a unique cross-talk among MCs, IL-10⁺ B_{reg} cells, and IL-13⁺ ILC2s could occur most possibly in the draining LNs.

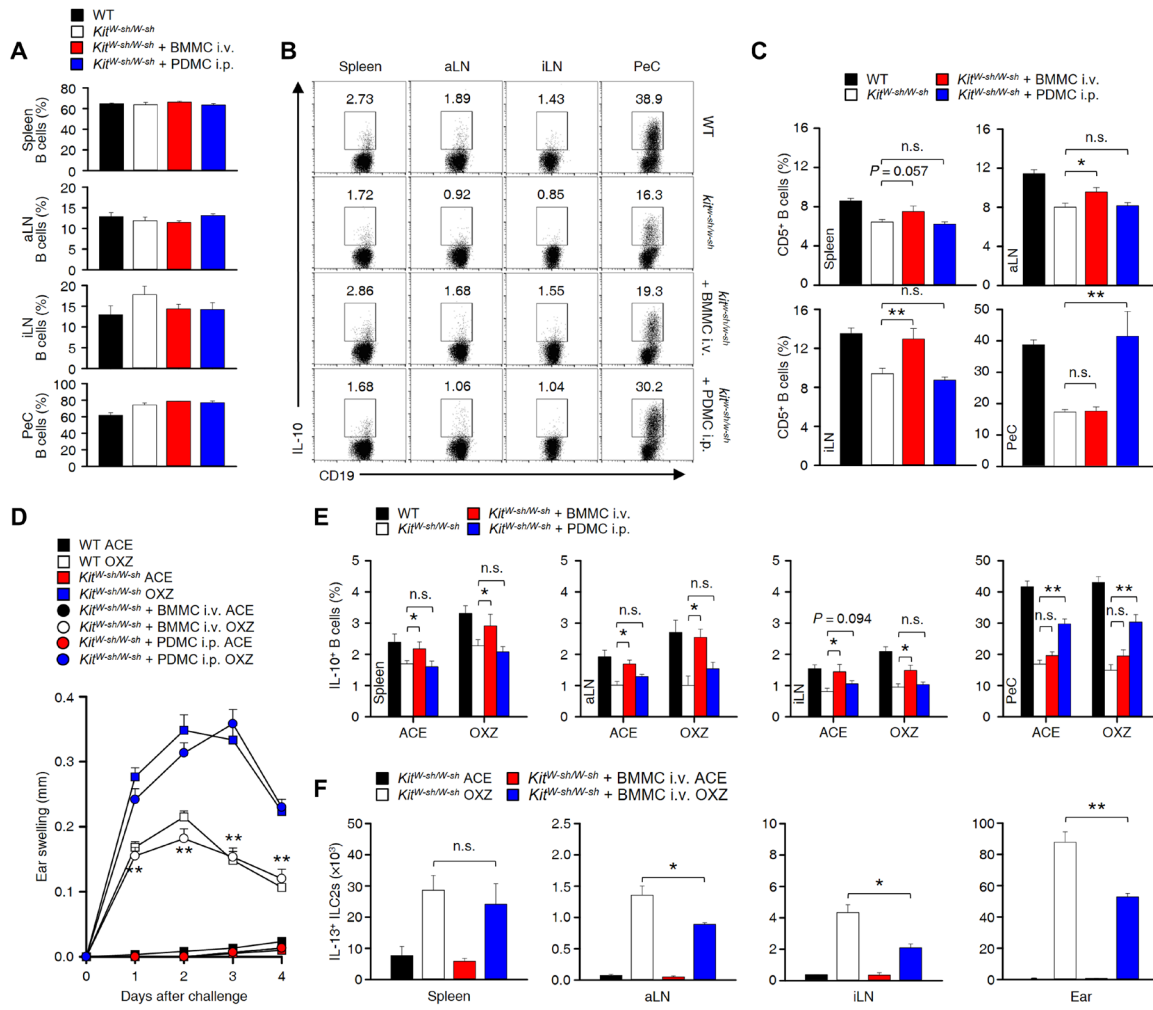


Fig. 4. Reconstitution of MCs in Kit^{W-sh/W-sh} mice increases IL-10⁺ B_{reg} cells and suppresses the CHS response. (A) The histograms show the frequencies of total CD19⁺ B cells in peripheral tissues from WT mice or Kit^{W-sh/W-sh} mice with or without the adoptive transfer of MCs. (B and C) Representative plot images show IL-10⁺ CD19⁺ B cells (B), and histograms show the frequencies of CD5⁺CD19⁺ B cells (C) in peripheral tissues from WT mice or Kit^{W-sh/W-sh} mice with or without the adoptive transfer of MCs. (D) Ear thickness, (E) the frequency of IL-10⁺ B cells, and (F) the number of IL-13⁺ ILC2s are shown during CHS in WT or Kit^{W-sh/W-sh} mice with or without the transfer of MCs. Data are expressed as the mean \pm SEM (A and C to F) and representative images (B) from two independent experiments ($n \geq 3$ per group for each experiment). * $P < 0.05$; ** $P < 0.01$; n.s., not significant by Student's t test (D and F) or one-way ANOVA with post hoc Tukey's test (C and E). BMMC, bone marrow-derived MC; PDMC, PeC-derived MC.

MC-derived IL-5 is critical for IL-10⁺ B_{reg} cell development

It was reported that MCs enhance the population of IL-10⁺ B_{reg} cells in IgE-mediated anaphylaxis and colitis through the interaction of CD40 (on B cells) and CD40L (on MCs) (9, 10). When Kit^{W-sh/W-sh} mice were reconstituted with Cd40L^{-/-} MCs, the CHS response was still inhibited similarly, if any, marginal, to the response in mice reconstituted with WT MCs, suggesting that the CHS response does not require the direct interaction of CD40 (B cells) and CD40L (MCs) unlike that in IgE-mediated anaphylaxis or colitis (fig. S7). We next measured changes in typical T_H1 and T_H2 cytokines in peripheral tissues, such as the serum, spleen, LNs, and ear, in WT and Kit^{W-sh/W-sh} mice. The amount of IL-5 was notably decreased in the LNs of Kit^{W-sh/W-sh} mice compared to that in the LNs of WT mice (fig. S8). Consistent with this finding, when we reconstituted MCs in Kit^{W-sh/W-sh} mice, the amount of IL-5 was increased in the LNs (Fig. 5A). Furthermore, IL-5 increased the population of IL-10⁺ B_{reg} cells and IL-10 secretion from CD19⁺ B cells (Fig. 5B). Previously, it was reported that IL-4 stimulated the expression of IL-5 receptors in B cells (25). We also

examined the expression of the IL-5 receptor, which was significantly increased by IL-4 (Fig. 5C). Next, during simultaneous treatment with IL-4 and IL-5 in CD19⁺ B cells, the population of IL-10⁺ B_{reg} cells and IL-10 secretion increased synergistically (Fig. 5D). These results suggest that MC IL-5 stimulates the development of IL-10⁺ B_{reg} cells through the activation of IL-5 receptor signaling in B_{reg} precursor cells.

Although the knowledge about the differentiation process of B_{reg} cells is very limited at present, IL-10⁺ B_{reg} cells are known to be the most abundant of the CD5⁺ B cell subsets, at least in mice (26). Furthermore, we found that MCs are critical for the development of CD5⁺ B cells (Fig. 4B). Next, we analyzed what type of CD5⁺ B cell subset was promoted by IL-5. IL-5 increased the expression of CD5 on CD19⁺ B cells (Fig. 5E). Furthermore, the simultaneous treatment with IL-4 and IL-5 synergistically increased the expression of CD5 (Fig. 5E). Yanaba *et al.* (21) reported that the frequency of IL-10⁺ B_{reg} cells was higher in the CD1d^{hi}CD5⁺ B cell subset than in other B cell subsets. However, Matsushita *et al.* (27) recently reported that

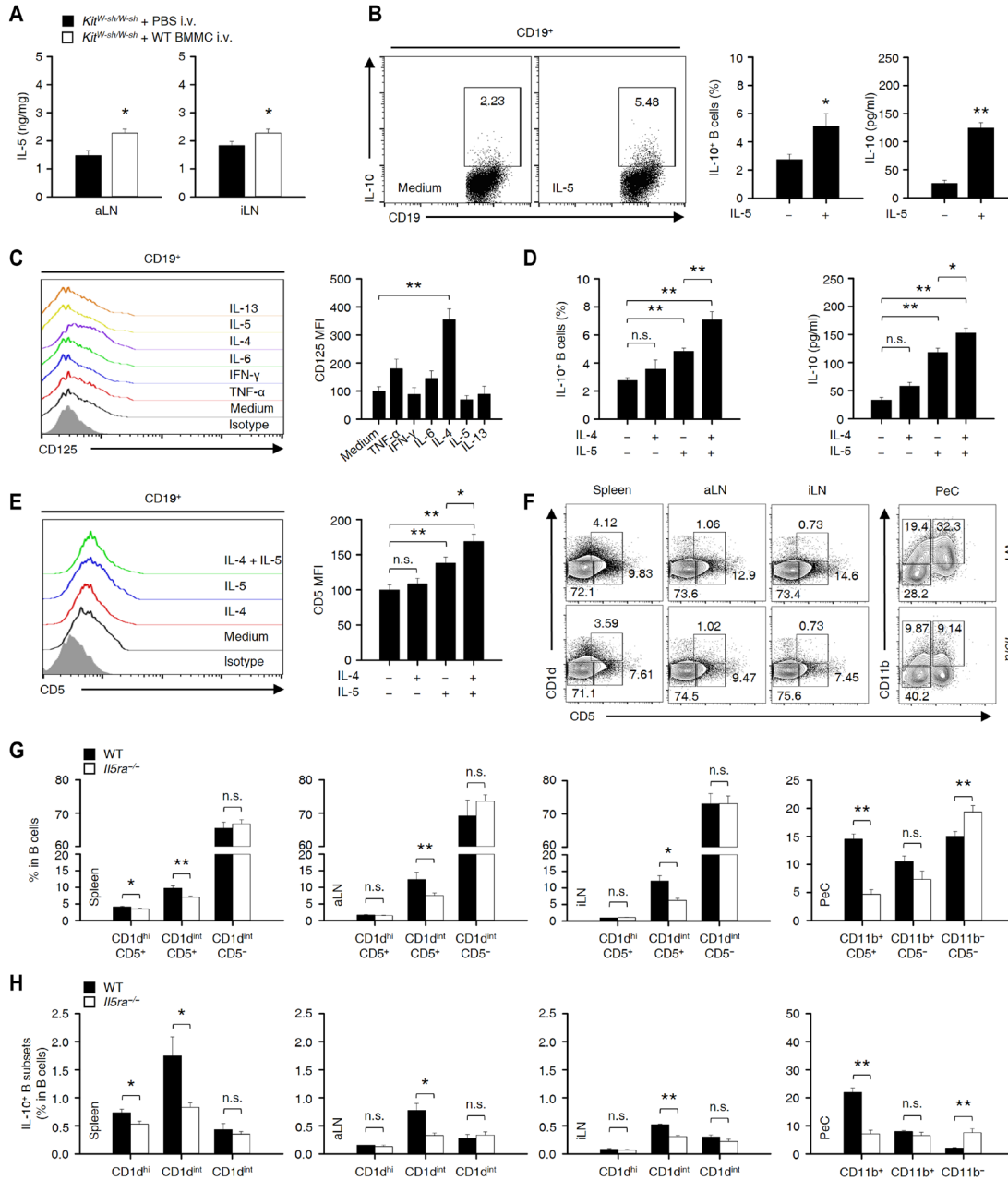


Fig. 5. IL-5-mediated signaling is critical for the development of CD1d^{int}CD5⁺ B_{reg} precursor cells and IL-10⁺ B_{reg} cells. (A) The histograms show the amount of IL-5 in LNs from Kit^{W-sh/W-sh} mice with or without the reconstitution of BMMCs. The data are expressed as the mean \pm SEM from three independent experiments ($n \geq 3$ per group for each experiment). * $P < 0.05$ versus phosphate-buffered saline (PBS) intravenous group by Student's *t* test. (B) Representative flow cytometry images (middle) and histograms for the population of IL-10⁺ B cells and the amount of IL-10 in the culture medium (right) are shown. Data are expressed as the mean \pm SEM from four independent experiments (triplicate for each experiment). * $P < 0.05$, ** $P < 0.01$ versus medium group by Student's *t* test. (C) Splenic CD19⁺ B cells (2×10^6 cells per well) from WT mice were cultured with or without cytokines [TNF- α , 10 ng/ml; IFN- γ (interferon- γ), 10 ng/ml; IL-6, 10 ng/ml; IL-4, 5 ng/ml; IL-5, 10 ng/ml; and IL-13, 100 ng/ml] for 48 hours. Representative flow cytometry images (left) and histograms (right) show the mean fluorescence intensity (MFI) of CD125 (IL-5Ra) on B cells. The results are expressed as representative images (left) and the mean \pm SEM (right) from three independent experiments (duplicate for each experiment). ** $P < 0.01$ versus medium group by Student's *t* test. (D) CD19⁺ B cells were stimulated with IL-4 (5 ng/ml), IL-5 (10 ng/ml), or IL-4 (5 ng/ml) + IL-5 (10 ng/ml) for 43 hours and subsequently stimulated with lipopolysaccharide (LPS) + phorbol 12-myristate 13-acetate (PMA), ionomycin, and monensin (PIM) for additional 5 hours. The histograms of IL-10⁺ B cells by flow cytometry (left) and the amount of IL-10 in the culture medium (right) are shown. (E) CD19⁺ B cells (2×10^6 cells per well) were cultured with or without IL-4 and IL-5 for 43 hours and subsequently stimulated with LPIM for 5 hours. Representative flow cytometry images (left) and histograms (right) show the MFIs of CD5 on B cells. (D and E) The results are expressed as the mean \pm SEM from three independent experiments (triplicate for each experiment). * $P < 0.05$; ** $P < 0.01$; n.s., not significant by one-way ANOVA with post hoc Tukey's test. (F to H) Representative flow cytometry images are shown for various B cell subsets (F), and histograms show the frequencies of the B cell subsets (G) and IL-10⁺ B cells (H) in peripheral tissues from WT or Il5ra^{-/-} mice. Data are expressed as the mean \pm SEM from three independent experiments ($n \geq 3$ per group for each experiment). * $P < 0.05$; ** $P < 0.01$; n.s., not significant versus WT by Student's *t* test.

IL-10^+ B_{reg} cells were more abundant in the $\text{CD1d}^{\text{int}}\text{CD5}^+$ B cell subset than in the $\text{CD1d}^{\text{hi}}\text{CD5}^+$ cell subset. Therefore, we measured the population changes of the $\text{CD1d}^{\text{hi}}\text{CD5}^+$, $\text{CD1d}^{\text{int}}\text{CD5}^+$, and $\text{CD1d}^{\text{int}}\text{CD5}^-$ B cell subsets in WT and $\text{Il5ra}^{-/-}$ mice. Notably, the $\text{CD1d}^{\text{int}}\text{CD5}^+$ (in the spleen and LNs) and $\text{CD11b}^+\text{CD5}^+$ (in the PeC) B cell subsets were remarkably suppressed in $\text{Il5ra}^{-/-}$ mice compared to those in WT mice (Fig. 5, F and G). The population of IL-10^+ B_{reg} cells was largely decreased in the $\text{CD1d}^{\text{int}}\text{CD5}^+$ B cells in $\text{Il5ra}^{-/-}$ mice, but the $\text{CD1d}^{\text{hi}}\text{CD5}^+$ and $\text{CD1d}^{\text{int}}\text{CD5}^-$ B cell subsets were marginally affected in $\text{Il5ra}^{-/-}$ mice compared to WT mice (Fig. 5H). The positive effect of IL-5 receptor signaling on the development of $\text{CD1d}^{\text{int}}\text{CD5}^+$ B cells or IL-10^+ B_{reg} cells was apparent in the LNs (Fig. 5, G and H), suggesting that IL-5 signaling is important for the development of IL-10^+ B_{reg} cells in the LNs.

MC IL-5 maintains the population of IL-10^+ B_{reg} cells in the LNs to suppress the CHS response

In cocultures of MCs and CD19^+ B cells, the population of IL-10^+ B_{reg} cells was significantly decreased by treatment with an antibody against the IL-5 receptor (Fig. 6, A and B). We further observed that the development of IL-10^+ B_{reg} cells was markedly reduced when $\text{Il5ra}^{-/-}$ B cells + WT MCs (Fig. 6C) or WT B cells + $\text{Il5}^{v/v}$ MCs were cocultured (Fig. 6D). Furthermore, when we reconstituted $\text{Il5}^{v/v}$ MCs in $\text{Kit}^{W-sh/W-sh}$ mice, minimal or no recovery of $\text{CD1d}^{\text{int}}\text{CD5}^+\text{CD19}^+$ B cells or the IL-10^+ B_{reg} population was observed (Fig. 6E); consistent with this result, the reconstitution of $\text{Il5}^{v/v}$ MCs did not inhibit IL-13^+ ILC2s (Fig. 6F) or CHS response in CHS mice (Fig. 6G). However, we could not find any difference in the distribution of engrafted WT and $\text{Il5}^{v/v}$ MCs (fig. S9, A and B). We further found out that the OXZ-induced CHS response was more severe in $\text{Il5ra}^{-/-}$ mice than in WT mice (Fig. 6H). However, the CHS response was significantly suppressed by the adoptive transfer of $\text{CD1d}^{\text{int}}\text{CD5}^+$ B cells but not $\text{Il5ra}^{-/-}$ $\text{CD1d}^{\text{int}}\text{CD5}^+$ B cells into CD19-deficient mice (Fig. 6I). No population change in the distribution of CD19^+ B cells in lymphoid tissues after the transfer of WT and $\text{Il5ra}^{-/-}$ $\text{CD1d}^{\text{int}}\text{CD5}^+$ B cells was observed (fig. S9, C and D). In $\text{Rag2}^{-/-}$ mice, the CHS response was also inhibited by the adoptive transfer of $\text{CD1d}^{\text{int}}\text{CD5}^+$ B cells but not $\text{Il5ra}^{-/-}$ $\text{CD1d}^{\text{int}}\text{CD5}^+$ B cells (Fig. 6J). Altogether, these results suggest that MC IL-5 is critical for maintaining IL-10^+ B_{reg} cells in peripheral lymphoid tissues.

DISCUSSION

In this study, we observed that the skin inflammation response induced by OXZ was much more severe in $\text{Kit}^{W-sh/W-sh}$ mice with CHS than in WT mice (Fig. 3A). However, when MCs were reconstituted intravenously in $\text{Kit}^{W-sh/W-sh}$ mice, CHS symptoms were alleviated to the level of WT mice (Fig. 4D). These results suggest that MCs are suppressive cells for skin inflammation in mice with hapten-induced CHS and chronic atopic dermatitis-like symptoms. We are also aware of the other abnormalities of MC-deficient $\text{Kit}^{W-sh/W-sh}$ mice caused by the lack of Kit (28–31). To overcome such a drawback, we carried out experiments by transferring various genetically modified or WT MCs (Fig. 6). Dudeck *et al.* reported some evidence that MCs amplify rather than limit CHS responses. They argued that the exaggerated CHS reactions, observed in Kit-mutant animals, are not caused by the absence of MCs but instead reflect other effects of the Kit deficiency (32). By contrast, Gimenez-Rivera *et al.* (16) and Reber *et al.* (17) recently reported that MCs suppress skin inflammation in

severe CHS based on findings in both Kit-mutant and Kit-independent MC-deficient mice. Furthermore, Reber *et al.* (17) have clearly shown that this controversy is due to the difference in the severity of CHS. Therefore, it is largely plausible that MCs function as a stimulator in mild CHS (32) or as a suppressor in severe CHS (Fig. 3A) (16, 17). In this study, B_{reg} cells were not fully recovered to the level of WT mice when MCs were reconstituted into $\text{Kit}^{W-sh/W-sh}$ mice, especially in PeC (Fig. 4E). Although our results demonstrated that MCs suppress the OXZ-induced severe CHS via the IL-10^+ B_{reg} cells, the possibility that Kit-dependent abnormalities of MCs would partially affect the regulator role of MCs should be considered.

MCs secrete a variety of biologically active substances, including many types of cytokines and chemokines (8). Recently, it was reported that MC IL-2 is helpful in stimulating the population of Foxp3^+ T_{reg} cells to suppress OXZ-induced skin inflammation (15). In $\text{Kit}^{W-sh/W-sh}$ mice, the IL-10^+ B_{reg} cell population was markedly decreased (Fig. 3, C and D), but the populations of Foxp3^+ T_{reg} cells and IL-10^+ Tr1 cells did not change (fig. S6, E and F), suggesting that there is another mechanism by which MCs suppress CHS symptoms in mice via regulation of the IL-10^+ B_{reg} cell population. Previously, we reported that MCs increased the IL-10^+ B_{reg} cell population through the interaction of CD40L (on MCs) and CD40 (on B_{reg} precursor cells) in the IgE-mediated acute allergic response (9). However, we observed in this study that the reconstitution of $\text{Cd40l}^{-/-}$ MCs in $\text{Kit}^{W-sh/W-sh}$ mice still suppressed the symptoms of CHS (fig. S7). Furthermore, in $\text{Kit}^{W-sh/W-sh}$ mice, the IL-10^+ B_{reg} cell population was markedly decreased (Fig. 3, C and D). These results suggest that there is another mechanism by which MCs maintain the population of IL-10^+ B_{reg} cells in CHS. In further experiments, we found that the amount of IL-5 was significantly reduced in LNs from $\text{Kit}^{W-sh/W-sh}$ mice compared to that in LNs from WT mice (fig. S8). When we transferred MCs intravenously into $\text{Kit}^{W-sh/W-sh}$ mice, IL-5 in LNs was recovered to the level of WT mice (Fig. 5A). These results suggest that MCs play an important role in maintaining a constant amount of IL-5 in the LNs. In addition, the IL-10^+ B_{reg} cell population was increased by IL-5 stimulation in CD19^+ B cells (Fig. 5B). Our results (Fig. 5C) and a previous report indicated that IL-4 increases the expression of the IL-5 receptor (CD125) on B cells (25). When CD19^+ B cells were treated with IL-4 and IL-5 simultaneously, the population of IL-10^+ B_{reg} cells was synergistically increased (Fig. 5D). Altogether, our results suggest that MCs are important for maintaining a constant level of IL-5 to maintain the homeostasis of IL-10^+ B_{reg} cells in peripheral lymphoid tissues, especially in the LNs.

ILC2s have been reported to be critical effector cells in skin inflammation, including atopic dermatitis (19, 24). We also observed that skin inflammation was significantly suppressed by the removal of all types of ILCs using a Thy1.2 mAb in $\text{Rag2}^{-/-}$ mice (Fig. 2E), suggesting that ILCs, most likely ILC2s, are the critical effector cells in OXZ-induced CHS. It has been well documented that IL-13 is critically associated with a variety of types of skin inflammation, and ILC2s are a major source of IL-13 in skin pathology (19). On the basis of our results and previous reports, we hypothesized that the aggravation of OXZ-induced CHS in $\text{Kit}^{W-sh/W-sh}$ mice was caused by the decrease in the IL-10^+ B_{reg} cell population and the subsequent reduced suppression of IL-13^+ ILC2s. We further observed that the transfer of MCs into $\text{Kit}^{W-sh/W-sh}$ mice restored the IL-10^+ B_{reg} cell population to the level of WT mice (Fig. 4). When MCs were transferred intravenously into $\text{Kit}^{W-sh/W-sh}$ mice, IL-10 $^+$ B_{reg} cells in the spleen and LNs but not in the PeC were restored to the levels of

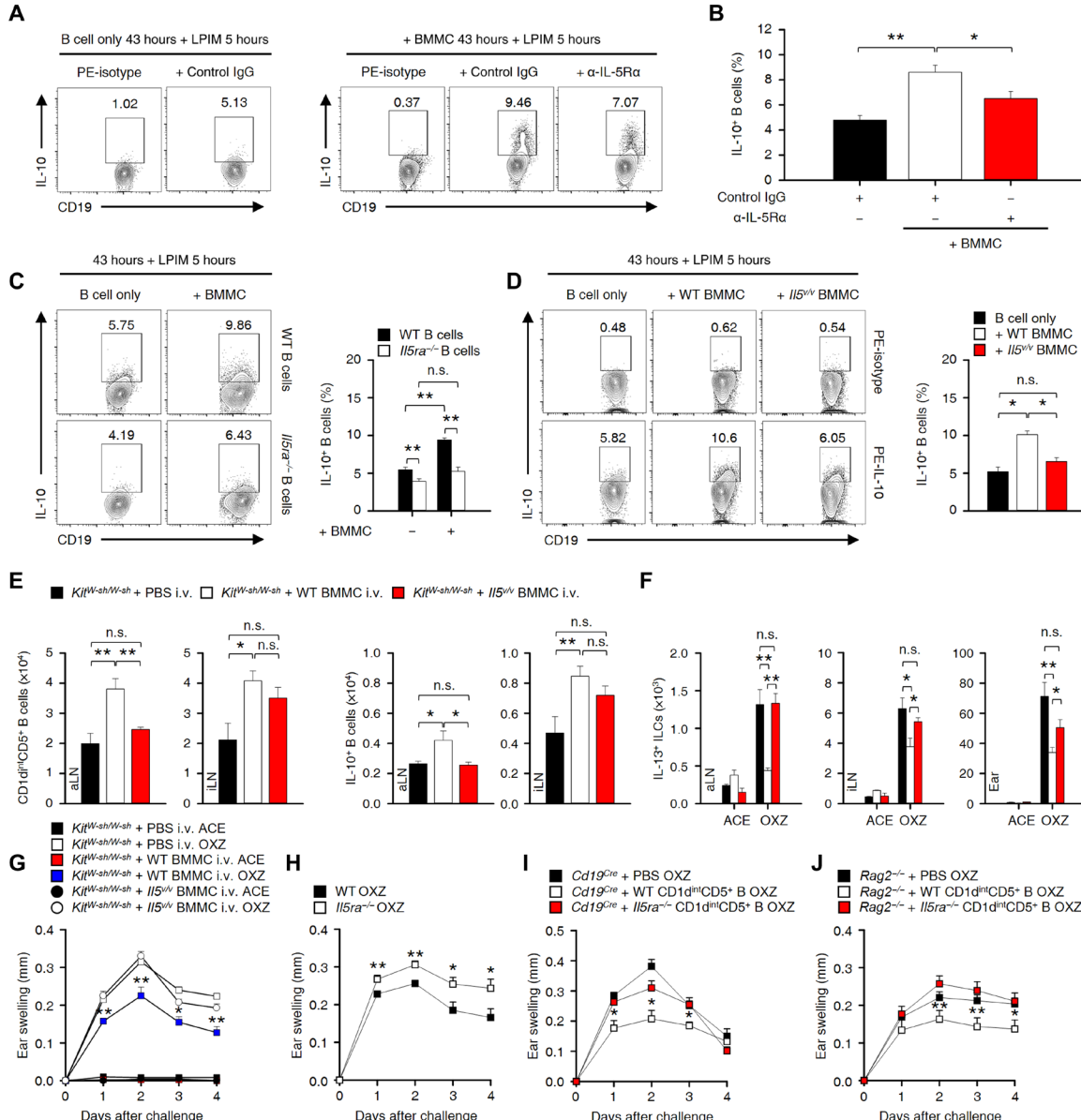


Fig. 6. MC-derived IL-5 is critical for the development of peripheral IL-10 $^{+}$ B cells to suppress CHS in mice. (A and B) Splenic CD19 $^{+}$ B cells (1.5 \times 10 6 cells per well) were cocultured with an equal number of BMMCs with an anti-IL-5R α mAb or isotype mAb for 43 hours and subsequently cultured with LPIM for 5 hours. Representative flow cytometry images (A) and histograms of the frequency of IL-10 $^{+}$ B cells (B) are shown. PE, phycoerythrin. (C and D) In (A) and (B), WT or $\text{II}5^{\text{VY}}$ splenic B cells were cocultured with equal numbers of WT or $\text{II}5^{\text{VY}}$ BMMCs as indicated. Representative flow cytometry images (left) and the frequency of IL-10 $^{+}$ B cells (right) are shown. (A to D) The results are expressed as representative images (A, C, and D) and mean \pm SEM (C and D) from three independent experiments (triplicate for each experiment). **P < 0.01 by one-way ANOVA with post hoc Tukey's test as indicated. (E and F) The histograms show the numbers of CD1d $^{\text{hi}}$ CD5 $^{+}$ B cells and IL-10 $^{+}$ B cells in LNs (E) or IL-13 $^{+}$ ILC2s in LNs and ear tissues (F) from $\text{Kit}^{\text{W-sh/W-sh}}$ mice with or without intravenous transfer of WT or $\text{II}5^{\text{VY}}$ BMMCs. (E and F) Data are expressed as the mean \pm SEM from three independent experiments ($n \geq 3$ per group for each experiment). *P < 0.05; **P < 0.01; n.s., not significant by one-way ANOVA with post hoc Tukey's test. (G) The graphs show the ear thicknesses of $\text{Kit}^{\text{W-sh/W-sh}}$ mice induced by OXZ with or without the reconstitution of WT or $\text{II}5^{\text{VY}}$ BMMCs. (H) The graphs show the ear thicknesses of WT or $\text{II}5^{\text{VY}}$ mice induced by OXZ with or without the transfer of WT or $\text{II}5^{\text{VY}}$ CD1d $^{\text{hi}}$ CD5 $^{+}$ B cells. (I to J) The graphs show the ear thicknesses of $\text{Cd}19^{\text{Cre}}$ mice (I) or $\text{Rag}2^{-/-}$ mice (J) induced by OXZ with or without the transfer of WT or $\text{II}5^{\text{VY}}$ CD1d $^{\text{hi}}$ CD5 $^{+}$ B cells. (G to J) Data are expressed as the mean \pm SEM from two independent experiments ($n \geq 3$ per group for each experiment). *P < 0.05, **P < 0.01 versus $\text{Kit}^{\text{W-sh/W-sh}}$ mice (G), WT mice (H), $\text{Cd}19^{\text{Cre}}$ mice (I), or $\text{Rag}2^{-/-}$ mice (J) by Student's t test.

WT mice, and IL-10 $^{+}$ B_{reg} cells were restored in the PeC only when PeC-derived MCs were transferred into the PeC (Fig. 4, B and E). Furthermore, OXZ-induced CHS was worse in $\text{Kit}^{\text{W-sh/W-sh}}$ mice than in WT mice, but the symptoms were greatly relieved by MC reconstitution via intravenous but not via intraperitoneal administration

(Fig. 4D). In particular, we found that IL-10 $^{+}$ B_{reg} cells specifically suppress the number of IL-13 $^{+}$ ILC2s in the LNs and ear tissues through adoptive transfer experiments with CD1d $^{\text{hi}}$ CD5 $^{+}$ B cells, including IL-10 $^{+}$ B_{reg} cells, in CD19-deficient mice (Fig. 2). The intravenous adoptive transfer of CD1d $^{\text{hi}}$ CD5 $^{+}$ B cells but not $\text{II}10^{-/-}$

CD1d^{hi}CD5⁺ B cells into *Rag2*^{-/-} recipient mice suppressed IL-13⁺ ILC2s in the ear tissue and LNs (Fig. 2, I and J), but we did not observe the migration of IL-10⁺ B_{reg} cells to the ear tissue (Fig. 2H). These results suggest that the lymphoid tissue in which IL-10⁺ B_{reg} cells regulate IL-13⁺ ILC2s is the LNs. Notably, the population of IL-13⁺ ILC2s and the amount of IL-13 were significantly increased in the LNs and ear tissue of *Kit*^{W-sh/W-sh} mice compared to those in WT mice (Fig. 3, E and F). We further observed that the CHS symptom was significantly suppressed when anti-IL-13 antibody was administered in the OXZ-induced mice with CHS (fig. S5). Collectively, it seems very likely that these elevated levels of IL-13 and IL-13⁺ ILC2s are the cause of worsening CHS symptoms. We further observed that the population of IL-13⁺ ILC2s was greatly suppressed by reconstituting MCs in *Kit*^{W-sh/W-sh} mice (Fig. 4F). Further, in vitro studies also demonstrated that B_{reg} cells suppressed the population of IL-13⁺ ILC2s in an IL-10-dependent manner (Fig. 2, K and L). These results suggest that MCs play an important role in maintaining the population of IL-10⁺ B_{reg} cells in the spleen and LNs to suppress skin inflammation via suppression of IL-13⁺ ILC2s.

B_{reg} cells have been characterized in the form of various phenotypes [CD19⁺CD1d^{hi}CD5⁺ (B10), CD19⁺CD5⁺ (B-1a), IgM^{hi}CD5⁺CD1d^{hi}FasL⁺, CD19⁺CD21^{hi}CD23^{hi}CD24^{hi}IgM^{hi}IgD^{hi}CD1d^{hi} (T2), CD19⁺CD21^{hi}CD23⁻ (MZ), CD138^{hi}PD-L1⁺B220⁺IgA⁺ (plasma cells), and others] (4, 33). Previous reports demonstrated that IL-10⁺ B_{reg} cells were mostly enriched in the CD1d^{hi}CD5⁺ B cell subset (21) or the CD1d^{int}CD5⁺ B cell subset (27). We observed that the adoptive transfer of MCs into *Kit*^{W-sh/W-sh} mice increased the CD5⁺ B cell subset population (Fig. 4C). In addition, treatment with IL-5 increased the expression of CD5 in B cells (Fig. 5E). Consistent with these findings, the population of the CD1d^{int}CD5⁺ B cell subset was significantly reduced in the peripheral lymphoid tissues of *Il5ra*^{-/-} mice (Fig. 5, G and H). Furthermore, in coculture experiments of WT MCs and B cells, the increase in the IL-10⁺ B_{reg} cell population by MCs was inhibited by blocking IL-5 signaling with an anti-IL-5 receptor antibody (Fig. 6, A and B). In addition, the increase in the IL-10⁺ B_{reg} cell population was not observed in coculture experiments of *Il5ra*^{-/-} B cells + WT MCs (Fig. 6C) or WT B cells + *Il5*^{V/V} MCs (Fig. 6D). These results suggested that the cross-talk between the IL-5 receptor on B cells and IL-5 from MCs is critical for the formation of IL-10⁺ B_{reg} cells in peripheral tissues. When we transferred *Il5*^{V/V} MCs intravenously into *Kit*^{W-sh/W-sh} mice, the increase in CD1d^{int}CD5⁺ B_{reg} precursor subsets and IL-10⁺ B_{reg} cells was not observed (Fig. 6, E and F). In addition, the inhibitory effect of MCs on CHS symptoms after the adoptive transfer of *Il5*^{V/V} MCs into *Kit*^{W-sh/W-sh} mice largely diminished compared to symptoms after the transfer of WT MCs (Fig. 6G). We also observed that the transfer of *Il5ra*^{-/-} CD1d^{int}CD5⁺ B cells into *Cd19*^{Cre} or *Rag2*^{-/-} mice failed to show a suppressive effect on CHS when compared with the transfer of WT CD1d^{int}CD5⁺ B cells (Fig. 6, I and J). Together, these results indicate that MC IL-5 has no effect or minor effects on the population of CD1d^{hi}CD5⁺ B_{reg} precursor cells but plays an important role in maintaining CD1d^{int}CD5⁺ B_{reg} precursor cells in the peripheral lymphoid tissues, especially in the LNs.

The mechanism of immune tolerance is critical for protecting the healthy body from abnormal and excessive immune responses. The destruction of immune tolerance may lead to autoimmune or allergic diseases (34). It is generally accepted that there are two pivotal mechanisms for obtaining central and peripheral immune tolerance. The mechanism of central tolerance is defined by the removal of

lymphocytes that respond to autoantigens called negative selection, when lymphocytes are developed in the bone marrow and thymus (35). When mature immune cells that pass central tolerance migrate to the peripheral tissues, immune cells that respond to autoantigens presented in the peripheral tissues are removed or inactivated by the mechanism of peripheral immune tolerance (36). Peripheral immune tolerance is developed in peripheral lymphoid tissues by intrinsic anergy and apoptosis of lymphocytes or by extrinsic regulatory immune cells, such as Foxp3⁺ T_{reg} cells (37). At present, the mechanism of central tolerance is relatively well established, whereas information about the mechanism that underlies peripheral immune tolerance is very limited. Our current results suggest that MCs are important for the homeostasis of IL-10⁺ B_{reg} cells in peripheral tissues in OXZ-induced severe CHS. In cooperation with Foxp3⁺ T_{reg} cells, IL-10⁺ B_{reg} cells can play an important role in maintaining immune tolerance in the periphery. Therefore, this study suggests that MC IL-5 may be a critical cytokine for peripheral immune tolerance via IL-10⁺ B_{reg} cells.

In this study, we demonstrated that MC IL-5 reduced the symptoms of OXZ-induced severe CHS by maintaining the population of IL-10⁺ B_{reg} cells in peripheral lymphoid tissues such as spleen and LNs (Fig. 6). However, studies on whether MC IL-5 has the same regulatory effect in CHS animal models induced by other haptens remain to be clear. For example, it was recently reported that MCs suppress the development of some severe CHS responses induced by 2,4-dinitrofluorobenzene (DNFB) by themselves producing IL-10, especially at early intervals after induction of the CHS (17). They also suggested that there would be other mechanisms besides the mechanism that MCs secrete IL-10. On the basis of their results and our present results, it is possible that the MC production of both IL-10 and IL-5 has a cooperative role in regulating the severity of CHS by various haptens, including DNFB and OXZ.

In summary, we demonstrate that MC IL-5 is important for maintaining the homeostasis of IL-10⁺ B_{reg} cells in peripheral lymphoid tissues in OXZ-induced severe CHS. The B_{reg} cells inhibit IL-13⁺ ILC2s to suppress skin inflammation in an IL-10-dependent manner.

MATERIALS AND METHODS

Mice

WT (6- to 10-week-old male C57BL/6 mice), *Cd19*^{Cre} (CD19 deficient), *Il10*^{-/-}, *Rag2*^{-/-}, *Cd40l*^{-/-}, and *Kit*^{W-sh/W-sh} mice on the C57BL/6 background were purchased from The Jackson Laboratory (Bar Harbor, ME). *Il5ra*^{-/-} (C57BL/6 background) mice were obtained from the RIKEN BioResource Center (Tsukuba, Japan). *Il5*^{V/V} knock-in (C57BL/6 background; IL-5 deficient) mice were provided by S. Takaki (Department of Immune Regulation, Research Institute, National Center for Global Health and Medicine, Chiba, Japan), and the mice were generated as previously described (38). The mice were housed in a pathogen-free facility at Konkuk University (Seoul, Korea).

Induction of a CHS mouse model

CHS was induced according to a previously reported method (21). Briefly, the mice were sensitized with 25 μ l of OXZ (100 mg/ml; Sigma-Aldrich, St. Louis, MO) in acetone/olive oil (4:1, v/v) on the shaved hind flank for two consecutive days. Five days later, the mice were challenged by the application of 10 μ l of OXZ (10 mg/ml) in acetone/olive oil (4:1, v/v) on the ear. Ear thickness was measured by two blinded independent observers. Two days after the mice were

challenged with OXZ, the lymphoid tissues were isolated and used for flow cytometric analysis or enzyme-linked immunosorbent assay (ELISA).

In vivo antibody-based neutralization

To deplete ILCs in vivo, the *Rag2*^{-/-} mice were injected intraperitoneally with 200 µg of an anti-Thy1.2 mAb (30H12, Bio X Cell, West Lebanon, NH) or isotype-matched control mAb three times on day -5 (sensitization), day -2 (before challenge), and day 1 (after challenge). For the depletion of T_{reg} cells, the *Cd19*^{Cre} mice were also injected intraperitoneally with 250 µg of anti-CD25 mAb (PC61, Bio X Cell, West Lebanon, NH) or an isotype-matched control mAb twice on day -5 (sensitization) and day -1 (before challenge). To deplete IL-13, C57BL/6 mice were injected with 200 µg of anti-IL-13 mAb (8H8, InvivoGen, San Diego, CA) or an isotype-matched control mAb through the lateral tail vein twice on day -1 (before challenge) and day 0 (1 hour before challenge).

Histological analysis and immunofluorescence

After the induction of CHS, the fixed [4% paraformaldehyde in phosphate-buffered saline (PBS)] ear tissues were dehydrated in a graded ethanol series (70 to 100%), rinsed three times with xylene for 3 min each, and then embedded in paraffin. The 5-µm paraffin sections were stained with hematoxylin and eosin (H&E). MCs in the lymphoid tissues (e.g., spleen, aLN, and iLN) or ear tissues were histologically examined, as described previously (9). The number of MCs in each tissue was measured by toluidine blue staining. To determine IL-10⁺ B cells in tissues, the tissue sections were blocked with 10% normal horse serum for 1 hour and then stained with anti-IL-10 (1 µg/ml; A-2, Santa Cruz Biotechnology, Dallas, TX), anti-CD19 (1 µg/ml; eBio1D3, eBioscience, San Diego, CA), or B220-eFluor 570 (1 µg/ml; RA3-6B2, eBioscience) antibodies or isotype controls. After washing with PBS, the sections were incubated with fluorescein isothiocyanate-conjugated anti-mouse or anti-rat antibodies and then counterstained with 4',6'-diamidino-2-phenylindole. After mounting, fluorescence images were obtained using an FV-1000 laser scanning inverted confocal microscope (Olympus, Tokyo, Japan).

Preparation of B cell subsets, bone marrow-derived MCs, and PeC-derived MCs

Mouse splenic B cells were presorted by CD19 mAb-microbeads (Miltenyi Biotec, Bergisch Gladbach, Germany). CD1d^{hi}CD5⁺, CD1d^{int}CD5⁺, or CD1d^{int}CD5⁻ (non-B_{reg} cells) B cells were subsequently sorted by a FACSAria system (BD Biosciences) (fig. S10A). For adoptive transfer, each B cell subset (1.5×10^6 cells/0.2 ml of PBS) was transferred intravenously into recipient mice 48 hours before challenge with OXZ to induce CHS. For the reconstitution of MCs in *Kit*^{W-sh/W-sh} mice, bone marrow-derived MCs (BMMCs) from isolated C57BL/6 mice were cultured in complete RPMI 1640 medium containing IL-3 (10 ng/ml; PeproTech Inc., Rock Hill, NJ) for 4 weeks, following the published procedure (39). PeC-derived MCs (PDMCs) were cultured in complete RPMI 1640 medium containing IL-3 (10 ng/ml) and stem cell factor (30 ng/ml; PeproTech Inc., Rock Hill, NJ). After 48 hours, nonadherent cells were removed and replaced by the fresh complete medium for 9 days (40). The expression of c-Kit and Fc ϵ RI on BMMCs and PDMCs was analyzed with a FACSCanto II flow cytometer (BD Bioscience). BMMCs and PDMCs with a purity of more than 98% were used for the adoptive transfer experiments. BMMCs (1×10^7 cells per mouse, i.v., 8 weeks before

challenge) or PDMCs (5×10^6 cells per mouse, i.p., 4 weeks before challenge) were injected into recipient *Kit*^{W-sh/W-sh} mice.

Flow cytometric analysis

Single-cell suspensions were isolated from the spleen, aLN, iLN, PeC, and ear. Before cell surface markers were stained, Fc γ receptors were blocked with anti-CD16 and anti-CD32 mAbs (2.4G2, BD Biosciences), and conjugated and dead cells were excluded by analysis on the basis of forward and side light scatter parameters and staining with a LIVE/DEAD fixable dead cell stain kit (Life Technologies, Eugene, OR). The antibodies against surface proteins were as follows: Antibodies against IgM (eB121-15F9), IgD (11-26), CD1d (1B1), CD4 (RM4-5), CD5 (53-7.3), CD11b (M1/70), CD11c (N418), CD19 (eBio1D3), CD21/CD35 (eBioBD9), CD23 (B3B4), CD25 (PC61.5), CD40 (HM40-3), B220 (RA3-6B2), c-Kit (2B8), Fc ϵ RI (MAR-1), Sca-1 (D7), Gr-1 (RB6-8CS), F4/80 (BM8), and MHCII (M5/114.15.2) were obtained from eBioscience. Antibodies for CD3 (17A2), CD45 (30-F11), and CD127 (A7R34) were obtained from BioLegend (San Diego, CA). An anti-CD125 (T21) antibody and a hematopoietic lineage antibody cocktail [CD3e (145-2C11), CD11b (M1/70), B220 (RA3-6B2), Ly-76 (TER-119), Ly-6C, and Ly-6G (RB6-8C5)] were purchased from BD Biosciences. Antibodies for intracellular staining of IL-10 (JES5-16E3), IL-13 (eBio13A), IFN- γ (interferon- γ) (XMG1.2), IL-4 (11B11), IL-5 (TRFK5), or Foxp3 (FJK-16s), and a fixation/permeabilization kit were from eBioscience. For the detection of IL-10⁺ B cells isolated from each tissue, the isolated cells were stimulated with lipopolysaccharide (LPS; 10 µg/ml; Sigma-Aldrich), phorbol 12-myristate 13-acetate (PMA; 50 ng/ml; Sigma-Aldrich), ionomycin (500 ng/ml; Sigma), and monensin (2 µM; eBioscience) for 5 hours. For the analysis of IL-5-induced IL-10⁺ B_{reg} cells, splenic B cells were isolated by CD19 mAb-microbeads (Miltenyi Biotec). The CD19⁺ B cells (2×10^6 cells per well, 24-well plate) were stimulated with or without recombinant mouse IL-5 (10 ng/ml; PeproTech Inc., Rock Hill, NJ) for 43 hours and with PMA, ionomycin, and monensin (PIM) for an additional 5 hours. For the flow cytometric analysis of IL-13⁺ ILCs (Lin⁻CD45⁺CD127⁺Sca-1⁺) (fig. S10B), Foxp3⁺ T_{reg} cells (CD3⁺CD4⁺CD25⁺), and IFN- γ ⁺/IL-4⁺ T_H (CD3⁺CD4⁺) cells, the cells were stimulated with PMA (50 ng/ml; Sigma-Aldrich), ionomycin (500 ng/ml; Sigma), and brefeldin A (3 µg/ml; eBioscience) for 4 hours before analysis. The cells were then analyzed with a FACSCanto II flow cytometer (BD Bioscience) and FlowJo version 10 software (Tree Star, Ashland, OR).

Measurement of cytokines and IgS

Proteins from the peripheral tissues (e.g., spleen, aLN, iLN, and ear) of mice were isolated with 500 µl of complete extraction buffer (Abcam, Cambridge, MA) with homogenization. The level of cytokines was measured by using a mouse BD OptEIA ELISA kit according to the manufacturer's instructions (BD Biosciences, San Jose, CA). In some experiments, isolated splenic CD19⁺ B cells were stimulated with recombinant mouse IL-5 (10 ng/ml; PeproTech Inc., Rock Hill, NJ) for 48 hours. The level of IL-10 was assessed by using ELISA kits from BD Biosciences. The serum concentrations of IgG1, IgG2a, IgA, or IgE were measured using sandwich ELISAs (MaxiSorp, Nunc, Roskilde, Denmark). Briefly, a microtiter plate was coated with each Ig-specific capture antibody (BD Biosciences) overnight at 4°C. The plates were blocked with PBS buffer (pH 7.0) containing 10% fetal bovine serum. Sera were added to the wells and incubated at room temperature (RT) for 2 hours. The wells were washed and incubated

with 2 µg of biotin-labeled rat anti-mouse IgG1, IgG2a, IgA, or IgE (BD Biosciences) at RT for 1 hour. The supernatants were aspirated, and the wells were washed three times with a blocking buffer. The plates were incubated with a solution of streptavidin–horseradish peroxidase (BD Biosciences) at RT for 30 min. After washing out the solution, the plates were developed using a tetramethylbenzidine substrate solution (GenDEPOT, Barker, TX) and read at 450 nm.

In vitro coculture of B cells with MCs or ILC2s

Mouse B cells were isolated from splenocytes with CD19 mAb-microbeads (Miltenyi Biotec). Bone marrow–derived ILC2s were negatively selected by hematopoietic lineage cocktail mAb-microbeads (Miltenyi Biotec), and the cells were then incubated with IL-2, IL-25, and IL-33 (10 ng/ml) at 37°C for 72 hours. ILC2s were identified as the live hematopoietic lineage CD45⁺CD127⁺Sca-1⁺CD25⁺ subset by flow cytometry. The purity of the cells was more than 95%. Splenic B cells (1.5×10^6 cells) were cocultured with equal numbers of BMMCs or ILC2s at 37°C for 48 hours. For analysis of the frequency of IL-10-producing B cells, the cocultured B cells were stimulated with LPS + PIM for the last 5 hours and then subjected to the flow cytometric analysis.

Statistical analysis

The data are presented as the mean \pm SEM from three or more independent experiments for in vitro experiments. All animal experiments were performed with five or more mice per group in each experiment. Statistical analysis was done by Student's *t* test or the Mann-Whitney test. One-way analysis of variance (ANOVA) with Tukey's post hoc test was performed for comparisons among multiple experimental groups. Statistical analysis (**P* < 0.05 and ***P* < 0.01) was carried out with SigmaStat software version 12 (Systat Software, Inc., Point Richmond, CA).

Study approval

All animal experiments were approved by the Institutional Animal Care and Use Committee of Konkuk University.

SUPPLEMENTARY MATERIALS

Supplementary material for this article is available at <http://advances.sciencemag.org/cgi/content/full/5/7/eaav8152/DC1>

Fig. S1. Leukocyte population changes in mice with OXZ-induced CHS.

Fig. S2. T_{reg} cells are not essential for the development of IL-10⁺ B_{reg} cells in peripheral tissues.

Fig. S3. The population changes in MCs, IL-13⁺ ILC2s, and IL-10⁺ B_{reg} cells during OXZ-induced chronic atopic dermatitis (AD)-like skin inflammation.

Fig. S4. Comparison of MCs and T_{reg} cells in WT and Cd19^{Cre} mice with CHS.

Fig. S5. The treatment of IL-13 mAb suppresses OXZ-induced CHS in mice.

Fig. S6. Analysis of B cells, T_{reg} cells, and serum antibody isotypes from WT or Kit^{W-sh/W-sh} mice.

Fig. S7. CD40L on MCs is not critical for the suppression of CHS.

Fig. S8. Amounts of T_H1 and T_H2 cytokines in peripheral tissues from WT or Kit^{W-sh/W-sh} mice.

Fig. S9. The tissue distribution of MCs in Kit^{W-sh/W-sh} mice and B_{reg} cells in Cd19^{Cre} mice after the adoptive transfer of each cell.

Fig. S10. The sorting strategies for B cell subsets, IL-13⁺ ILC2s, and IL-10⁺ B cells.

REFERENCES AND NOTES

- T. W. LeBien, T. F. Tedder, B lymphocytes: How they develop and function. *Blood* **112**, 1570–1580 (2008).
- S. I. Katz, D. Parker, J. L. Turk, B-cell suppression of delayed hypersensitivity reactions. *Nature* **251**, 550–551 (1974).
- A. Mizoguchi, A. K. Bhan, A case for regulatory B cells. *J. Immunol.* **176**, 705–710 (2006).
- W. van de Veen, B. Stanic, O. F. Witz, K. Jansen, A. Globinska, M. Akdis, Role of regulatory B cells in immune tolerance to allergens and beyond. *J. Allergy Clin. Immunol.* **138**, 654–665 (2016).
- P. Natarajan, A. Singh, J. T. McNamara, E. R. Secor Jr., L. A. Guernsey, R. S. Thrall, C. M. Schramm, Regulatory B cells from hilar lymph nodes of tolerant mice in a murine model of allergic airway disease are CD5+, express TGF-β, and co-localize with CD4+Foxp3+ T cells. *Mucosal Immunol.* **5**, 691–701 (2012).
- P. Shen, T. Roch, V. Lampropoulou, R. A. O'Connor, U. Stervbo, E. Hilgenberg, S. Ries, V. D. Dang, Y. Jaimes, C. Daridon, R. Li, L. Jouneau, P. Boudinot, S. Wilantri, I. Sakwa, Y. Miyazaki, M. D. Leech, R. C. McPherson, S. Wirtz, M. Neurath, K. Hoechli, E. Meini, A. Grützkau, J. R. Grün, K. Horn, A. A. Kühl, T. Dörner, A. Bar-Or, S. H. E. Kaufmann, S. M. Anderton, S. Fillatreau, IL-35-producing B cells are critical regulators of immunity during autoimmune and infectious diseases. *Nature* **507**, 366–370 (2014).
- A. R. Khan, E. Hams, A. Floudas, T. Sparwasser, C. T. Weaver, P. G. Fallon, PD-L1hi B cells are critical regulators of humoral immunity. *Nat. Commun.* **6**, 5997 (2015).
- S. J. Galli, M. Tsai, IgE and mast cells in allergic disease. *Nat. Med.* **18**, 693–704 (2012).
- H. S. Kim, A. R. Kim, D. K. Kim, H. W. Kim, Y. H. Park, G. H. Jang, B. Kim, Y. M. Park, J. S. You, H. S. Kim, M. A. Beaven, Y. M. Kim, W. S. Choi, Interleukin-10-producing CD5+ B cells inhibit mast cells during immunoglobulin E-mediated allergic responses. *Sci. Signal.* **8**, ra28 (2015).
- F. Mion, F. D'Inca, L. Danelli, B. Toffoletto, C. Guarnotta, B. Frossi, A. Burocchi, A. Rigoni, N. Gerdes, E. Lutgens, C. Tripodo, M. P. Colombo, J. Rivera, G. Vitale, C. E. Pucillo, Mast cells control the expansion and differentiation of IL-10-competent B cells. *J. Immunol.* **193**, 4568–4579 (2014).
- T. Honda, G. Egawa, S. Grabbe, K. Kabashima, Update of immune events in the murine contact hypersensitivity model: Toward the understanding of allergic contact dermatitis. *J. Invest. Dermatol.* **133**, 303–315 (2013).
- A. D. Christensen, C. Haase, Immunological mechanisms of contact hypersensitivity in mice. *APMIS* **120**, 1–27 (2012).
- M. Q. Man, Y. Hatano, S. H. Lee, M. Man, S. Chang, K. R. Feingold, D. Y. Leung, W. Holleran, Y. Uchida, P. M. Elias, Characterization of a hapten-induced, murine model with multiple features of atopic dermatitis: Structural, immunologic, and biochemical changes following single versus multiple oxazolone challenges. *J. Invest. Dermatol.* **128**, 79–86 (2008).
- M. A. Grimaldeston, S. Nakae, J. Kalesnikoff, M. Tsai, S. J. Galli, Mast cell-derived interleukin 10 limits skin pathology in contact dermatitis and chronic irradiation with ultraviolet B. *Nat. Immunol.* **8**, 1095–1104 (2007).
- A. Y. Hershko, R. Suzuki, N. Charles, D. Alvarez-Errico, J. L. Sargent, A. Laurence, J. Rivera, Mast cell interleukin-2 production contributes to suppression of chronic allergic dermatitis. *Immunity* **35**, 562–571 (2011).
- V. A. Gimenez-Rivera, F. Siebenhaar, C. Zimmermann, H. Siiskonen, M. Metz, M. Maurer, Mast cells limit the exacerbation of chronic allergic contact dermatitis in response to repeated allergen exposure. *J. Immunol.* **197**, 4240–4246 (2016).
- L. L. Reber, R. Sibilano, P. Starkl, A. Roers, M. A. Grimaldeston, M. Tsai, N. Gaudenzio, S. J. Galli, Imaging protective mast cells in living mice during severe contact hypersensitivity. *JCI Insight* **2**, e92900 (2017).
- P. Licona-Limón, L. K. Kim, N. W. Palm, R. A. Flavell, TH2, allergy and group 2 innate lymphoid cells. *Nat. Immunol.* **14**, 536–542 (2013).
- B. Roediger, R. Kyle, G. Le Gros, W. Weninger, Dermal group 2 innate lymphoid cells in atop dermatitis and allergy. *Curr. Opin. Immunol.* **31**, 108–114 (2014).
- A.-R. Kim, H. S. Kim, D. K. Kim, S. T. Nam, H. W. Kim, Y. H. Park, D. Lee, M. B. Lee, J. H. Lee, B. Kim, M. A. Beaven, H. S. Kim, Y. M. Kim, W. S. Choi, Mesenteric IL-10-producing CD5⁺ regulatory B cells suppress cow's milk casein-induced allergic responses in mice. *Sci. Rep.* **6**, 19685 (2016).
- K. Yanaba, J. D. Bouaziz, K. M. Haas, J. C. Poe, M. Fujimoto, T. F. Tedder, A regulatory B cell subset with a unique CD1dhiCD5⁺ phenotype controls T cell-dependent inflammatory responses. *Immunity* **28**, 639–650 (2008).
- H. Watanabe, M. Unger, B. Tuvel, B. Wang, D. N. Sauder, Contact hypersensitivity: The mechanism of immune responses and T cell balance. *J. Interferon Cytokine Res.* **22**, 407–412 (2002).
- Y. Shinkai, G. Rathbun, K. P. Lam, E. M. Oltz, V. Stewart, M. Mendelsohn, J. Charron, M. Datta, F. Young, A. M. Stall, RAG-2-deficient mice lack mature lymphocytes owing to inability to initiate V(D)J rearrangement. *Cell* **68**, 855–867 (1992).
- B. S. Kim, M. C. Siracusa, S. A. Saenz, M. Noti, L. A. Monticelli, G. F. Sonnenberg, M. R. Hepworth, A. S. Van Voorhees, M. R. Comeau, D. Artis, TSLP elicits IL-33-independent innate lymphoid cell responses to promote skin inflammation. *Sci. Transl. Med.* **5**, 170ra16 (2013).
- J. D. Weber, P. C. Isakson, J. M. Purkerson, IL-5 receptor expression and Ig secretion from murine B lymphocytes requires coordinated signaling by membrane Ig, IL-4, and IL-5. *J. Immunol.* **157**, 4428–4435 (1996).
- A. O'Garra, R. Chang, N. Go, R. Hastings, G. Haughton, M. Howard, Ly-1 B (B-1) cells are the main source of B cell-derived interleukin 10. *Eur. J. Immunol.* **22**, 711–717 (1992).
- T. Matsushita, D. Le Huu, T. Kobayashi, Y. Hamaguchi, M. Hasegawa, K. Naka, A. Hirota, M. Muramatsu, K. Takehara, M. Fujimoto, A novel splenic B1 regulatory cell subset suppresses allergic disease through phosphatidylinositol 3-kinase-Akt pathway activation. *J. Allergy Clin. Immunol.* **138**, 1170–1182.e9 (2016).
- L. L. Reber, T. Marichal, S. J. Galli, New models for analyzing mast cell functions in vivo. *Trends Immunol.* **33**, 613–625 (2012).

29. H. R. Rodewald, T. B. Feyerabend, Widespread immunological functions of mast cells: Fact or fiction? *Immunity* **37**, 13–24 (2012).
30. N. Gaudenzio, R. Sibilano, P. Starkl, M. Tsai, S. J. Galli, L. L. Reber, Analyzing the functions of mast cells in vivo using ‘mast cell knock-in’ mice. *J. Vis. Exp.* **99**, e52753 (2015).
31. M. A. Grimaldheston, C. C. Chen, A. M. Piliponsky, M. Tsai, S. Y. Tam, S. J. Galli, Mast cell-deficient W-sash c-kit mutant Kit W-sh/W-sh mice as a model for investigating mast cell biology in vivo. *Am. J. Pathol.* **167**, 835–848 (2005).
32. A. Dudeck, J. Dudeck, J. Scholten, A. Petzold, S. Surianarayanan, A. Köhler, K. Peschke, D. Vöhringer, C. Waskow, T. Krieg, W. Müller, A. Waisman, K. Hartmann, M. Gunzer, A. Roers, Mast cells are key promoters of contact allergy that mediate the adjuvant effects of haptens. *Immunity* **34**, 973–984 (2011).
33. E. C. Rosser, C. Mauri, Regulatory B cells: Origin, phenotype, and function. *Immunity* **42**, 607–612 (2015).
34. O. U. Soyer, M. Akdis, J. Ring, H. Behrendt, R. Crameri, R. Lauener, C. A. Akdis, Mechanisms of peripheral tolerance to allergens. *Allergy* **68**, 161–170 (2013).
35. T. K. Starr, S. C. Jameson, K. A. Hogquist, Positive and negative selection of T cells. *Annu. Rev. Immunol.* **21**, 139–176 (2003).
36. T. C. Metzger, M. S. Anderson, Control of central and peripheral tolerance by Aire. *Immunol. Rev.* **241**, 89–103 (2011).
37. S. Sakaguchi, K. Wing, T. Yamaguchi, Dynamics of peripheral tolerance and immune regulation mediated by Treg. *Eur. J. Immunol.* **39**, 2331–2336 (2009).
38. M. Ikuani, T. Yanagibashi, M. Ogasawara, K. Tsuneyama, S. Yamamoto, Y. Hattori, T. Kouro, A. Itakura, Y. Nagai, S. Takaki, K. Takatsu, Identification of innate IL-5-producing cells and their role in lung eosinophil regulation and antitumor immunity. *J. Immunol.* **188**, 703–713 (2012).
39. M. Rådinger, B. M. Jensen, H. S. Kuehn, A. Kirshenbaum, A. M. Gilfillan, Generation, isolation, and maintenance of human mast cells and mast cell lines derived from peripheral blood or cord blood. *Curr. Protoc. Immunol. Chapter 7*, Unit 7.37 (2010).
40. K. V. Vukman, T. Visnovitz, P. N. Adams, M. Metz, M. Maurer, S. M. O'Neill, Mast cells cultured from IL-3-treated mice show impaired responses to bacterial antigen stimulation. *Inflamm. Res.* **61**, 79–85 (2012).

Acknowledgments

Funding: This research was supported by a National Research Foundation of Korea (NRF) grant funded by the Korean government (NRF-2016R1A2B3015840 and NRF-2016R1A5A2012284 and in part by NRF-2017R1D1B03028379 and NRF-2013R1A4A1069575).

Author contributions: W.S.C. designed the experiments, interpreted the results, and wrote the paper. H.S.K. performed most of the experiments and wrote the draft manuscript. M.B.L. performed flow cytometry and molecular analysis. D.L., K.Y.M., and J.K. performed in vivo experiments and collected the data. Y.H.P. and H.W.K. performed histological analysis. S.J.K. analyzed in vitro data. M.I. and S.T. provided the knockout animals and analyzed and discussed the data. Y.M.K. provided intellectual input, discussed the results, and wrote the paper.

Competing interests: The authors declare that they have no competing interests. **Data and materials availability:** All data needed to evaluate the conclusions in the paper are present in the paper and/or the Supplementary Materials. Additional data related to this paper may be requested from the authors.

Submitted 23 October 2018

Accepted 10 June 2019

Published 17 July 2019

10.1126/sciadv.aav8152

Citation: H. S. Kim, M. B. Lee, D. Lee, K. Y. Min, J. Koo, H. W. Kim, Y. H. Park, S. J. Kim, M. Ikuani, S. Takaki, Y. M. Kim, W. S. Choi, The regulatory B cell-mediated peripheral tolerance maintained by mast cell IL-5 suppresses oxazolone-induced contact hypersensitivity. *Sci. Adv.* **5**, eaav8152 (2019).